Electrochemistry Communications 118 (2020) 106788

Contents lists available at ScienceDirect

Electrochemistry Communications

journal homepage: www.elsevier.com/locate/elecom

Anodization of electrodeposited titanium films towards TiO_2 nanotube layers

Hanna Sopha[a,b], Yutaro Norikawa[c], Martin Motola[a], Ludek Hromadko[a,b], Jhonatan Rodriguez-Pereira[a], Jiri Cerny[d], Toshiyuki Nohira[c], Kouji Yasuda[e,f,1], Jan M. Macak[a,b,*]

[a] Center of Materials and Nanotechnologies, Faculty of Chemical Technology, University of Pardubice, Nam. Cs. Legii 565, 53002 Pardubice, Czech Republic
[b] Central European Institute of Technology, Brno University of Technology, Purkyňova 123, 612 00 Brno, Czech Republic
[c] Institute of Advanced Energy, Kyoto University, Gokasho, Uji, Kyoto 611-0011, Japan
[d] Centre for Organic Chemistry, Rybitvi 296, 533 54 Rybitví, Czech Republic
[e] Agency for Health, Safety and Environment, Kyoto University, Yoshida-hommachi, Sakyo-ku, Kyoto 606-8501, Japan
[f] Department of Fundamental Energy Science, Graduate School of Energy Science, Kyoto University, Yoshida-hommachi, Sakyo-ku, Kyoto 606-8501, Japan

ARTICLE INFO

Keywords:
TiO_2
Nanotubes
electrodeposited Ti
Anodization
Photoelectrochemistry

ABSTRACT

Ti films electrodeposited on Ni foils from molten salts were anodized towards TiO_2 nanotube formation for the first time. The resulting TiO_2 nanotube (TNT) layers were compared with TNT layers prepared under identical conditions on Ti foils by means of scanning electron microscopy (SEM), X-ray diffraction (XRD) measurements, X-ray photoelectron spectroscopy (XPS), and photocurrent measurements. No significant differences were found between the TNT layers prepared on the two different substrates. Electrodeposited Ti films prepared in this way could thus be a viable option for anodization purposes.

1. Introduction

Within the last 17 years, anodic TiO_2 nanotube (TNT) layers have attracted enormous attention, due to the extraordinary physical and chemical properties of TiO_2 and owing to the specific advantages of aligned nanotube layers, such as large surface area, high surface-to-volume ratio, directional charge or ion transport, efficient electron-hole separation, size exclusion effects, and biological interactions [1]. They can be used in a plethora of applications, as described in various reviews [1–3].

Anodic TNT layers are prepared by anodization of Ti substrates in fluoride-containing electrolytes [4–7]. Many reports describing the production of TNT layers on several different kinds of Ti substrates can be found in the literature. The most commonly used Ti substrate is Ti foil with a thickness of between ~100 nm and ~200 nm, as these foils can easily be cut and leave a sufficient Ti back contact for applications. However, other Ti substrates are also frequently used for anodization, such as thick Ti sheets (1–2 mm thick) [8], Ti meshes [9–11], or thin magnetron sputtered Ti films on silicon [12,13], fluorine-doped tin oxide (FTO) [14,15], or indium tin oxide (ITO) [16,17]. In particular, TNT layers directly prepared on conductive transparent glasses, such as ITO or FTO, are interesting for photoelectrochemical applications, including solar cells [15,17] or photocatalytic H_2 production [14]. However, one disadvantage of these ITO or FTO substrates is that they are not smooth, and thus thin Ti films sputtered on these substrates are usually uneven. This in turn results in difficulties in their anodization, as within relatively short anodization times the thin Ti film is completely consumed at some small spots and the glass substrate is reached. As a result, TNT layers produced on sputtered Ti films on conductive glasses often have a porous oxide layer on top.

An alternative to sputtered Ti films is electrodeposited Ti films. Plating on substrates with complicated shapes is possible with electrodeposition. Ti can be electrodeposited in high-temperature molten salts, e.g. LiCl–KCl [18], NaCl–KCl [19], $CaCl_2$ [20], LiF–NaF–KF [21], or LiF–NaF–KF [22]. In particular, smooth Ti films can be deposited in fluoride-containing salts. However, due to the low water solubility of fluoride salts it is difficult to remove the solidified salt from the electrodeposited Ti films [23]. To solve this problem we recently proposed a new method for electrodeposition of Ti using a water soluble KF–KCl molten salt [23–25]. Using this method, smooth and dense Ti films with a thickness of ~15 μm were deposited on Ni electrodes, which are established substrates for this purpose [23–25].

* Corresponding author at: Center of Materials and Nanotechnologies, Faculty of Chemical Technology, University of Pardubice, Nam. Cs. Legii 565, 53002 Pardubice, Czech Republic.
E-mail address: jan.macak@upce.cz (J.M. Macak).
[1] Present address: Graduate School of Engineering, Kyoto University, Yoshida-honmachi, Sakyo-ku, Kyoto 606-8501, Japan.

https://doi.org/10.1016/j.elecom.2020.106788
Received 16 June 2020; Received in revised form 30 June 2020; Accepted 8 July 2020
Available online 13 July 2020

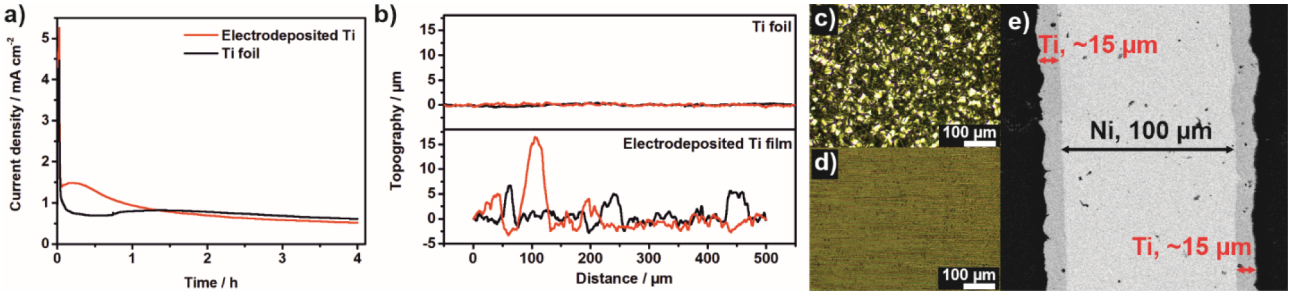

Fig. 1. (a) Current-time plots; (b) roughness profiles obtained by profilometry. Optical microscope images of (c) the electrodeposited Ti film and (d) the Ti foil, (e) cross-sectional SEM of the non-anodized electrodeposited Ti film on Ni substrate.

Interestingly, there has not yet been a study showing the anodization of the electrodeposited Ti films to produce TNT layers. Thus, in this communication the preparation of TNT layers on electrodeposited Ti films on Ni substrates is demonstrated for the first time. Using scanning electron microscopy (SEM), X-ray diffraction (XRD) measurements, X-ray photoelectron spectroscopy (XPS), and photocurrent measurements, the TNT layers prepared on electrodeposited Ti films are compared to TNT layers prepared on Ti foils.

2. Experimental

Ti films (approximately 15 µm) were galvanostatically electrodeposited on Ni substrates (Nilaco Corp., 20 mm × 20 mm, thickness: 0.1 mm) at -25 mA cm^{-2} for 40 min from molten KF–KCl salt (45:55 mol%) at 650 °C, containing 0.5 mol% K_2TiF_6 and 1.7 mol% Ti sponge (Kojundo Chemical Laboratory Co., Ltd.) [23–25]. The impurities of the electrodeposited Ti film were analyzed using inductively coupled plasma atomic emission spectroscopy (ICP-AES) to < 100 ppm.

Anodization of the electrodeposited Ti layer and a conventional Ti foil (Sigma-Aldrich, 99.7% purity, 127 µm thick) was carried out in an ethylene glycol-based electrolyte containing 0.15 M NH_4F and 10 vol% H_2O at 100 V for 4 h with an initial sweep of 1 V/s employing a high-voltage potentiostat (PGU-200 V, IPS Elektroniklabor GmbH), using the Ti substrate as the anode and a Pt foil as the cathode [26]. For a better comparison of the obtained TNT layers, electrolytes of exactly the same age were used for the anodization of both substrates [27].

The surface topography was measured using a mechanical profilometer (DektakXT, Bruker) at a length scale of 500 µm, with a step of 0.5 µm. A LEICA DM750M microscope equipped with a CCD camera and LAS software was used to obtain optical microscope images.

Photocurrent measurements were carried out using a photoelectric spectrophotometer (Instytut Fotonowy) with a 150 W Xe lamp and a monochromator with a bandwidth of 5 nm connected to a modular electrochemical system AUTOLAB (PGSTAT 204; Metrohm Autolab B. V.; Nova 1.10 software) in an aqueous 0.1 M Na_2SO_4 solution at 0.4 V vs. Ag/AgCl in the spectral range from 300 to 450 nm. The incident photon-to-electron conversion efficiency (IPCE) value for each wavelength was calculated as described in our previous work [26,28].

The morphology of the TNT layers was characterized by field-emission scanning electron microscopy (FE-SEM, JEOL JSM 7500F). To obtain cross-sectional images, the TNT layers were carefully scratched. The diameters and thicknesses were evaluated by statistical analysis of the SEM images using proprietary Nanomeasure software.

X-ray diffraction (XRD) patterns were measured with a Panalytical Empyrean diffractometer using a Cu X-ray tube and a scintillation detector Pixcel3D. The measurements were performed in the 2θ range 5–65°, step size 0.026°.

The composition of the TNT layers was monitored by X-ray photoelectron spectroscopy (XPS) (ESCA 2SR, Scienta-Omicron) using a monochromatic Al Kα (1486.7 eV) X-ray source. The binding energy scale was referenced to adventitious carbon (284.8 eV). The quantitative analysis was performed using the elemental sensitivity factors provided by the manufacturer.

3. Results and discussion

Fig. 1a shows the current–time plots recorded during the anodization process. As described in the literature [2], three different stages can be observed for both anodized Ti substrates: (i) a fast current decay due to the formation of an anodic flat oxide layer; (ii) a current increase attributed to the formation of pores within the oxide layer (increase in the surface area); and (iii) a slow current decay towards a steady-state while the nanotubes grow in length. The main difference between the current–time plots recorded on the two substrates is that the second stage is reached faster in the case of the electrodeposited Ti film compared to the Ti foil. Thus, pore formation starts earlier. A possible reason for this is that the surface of the electrodeposited Ti film is rougher than of the Ti foil. To test this, profilometric measurements were carried out on both Ti substrates, as shown in Fig. 1b, which provides roughness profiles parallel to the rolling lines (in the case of the Ti foil, black lines) and profiles in a perpendicular direction (red lines). In the case of the electrodeposited Ti film, the roughness was measured for two lines perpendicular to each other. The root mean square (RMS) values were 1922 nm and 106 nm for the electrodeposited Ti film and the Ti foil, respectively. This confirms the significantly higher roughness of the electrodeposited Ti film compared to the Ti foil due to grain growth during electrodeposition at a high temperature. The optical microscope images of the electrodeposited Ti film and the Ti foil are shown in Fig. 1c and 1d. A grain-like Ti structure can be seen for the electrodeposited Ti film while the Ti foil is rather smooth with clearly observable rolling lines due to the processing. This is additional proof of the greater roughness of the electrodeposited Ti film. Fig. 1e shows a cross-sectional SEM image of the electrodeposited Ti film, revealing an overall Ti film thickness of ~ 15 µm.

Fig. 2a and 2b show SEM images of the tops of the TNT layers produced on the electrodeposited Ti film and the Ti foil, respectively. The inner diameters are ~ 244 nm for the TNTs on the electrodeposited Ti film and ~ 223 nm for the TNTs on the Ti foil. It can be seen that the TNT tops on the electrodeposited Ti substrate have significantly thinner nanotube walls than the TNT tops on the Ti foil. This is attributed to stronger etching of the surface of the electrodeposited Ti film and is in accordance with the recorded current–time plots and the TNT layer thicknesses shown in Fig. 2c and d for the two Ti substrates (i.e. the TNT layer on the Ti foil is thinner than that on the electrodeposited Ti film). Thus, the stronger etching and decreased TNT layer thickness on the electrodeposited Ti film are attributed to the higher roughness of this substrate compared to the Ti foil.

Fig. 2e shows the XRD patterns recorded for the annealed TNT layers on both substrates. As expected, both TNT layers show only the anatase structure after annealing at 400 °C. The TNT layer on the electrodeposited Ti film shows anatase TiO_2 in a preferred orientation

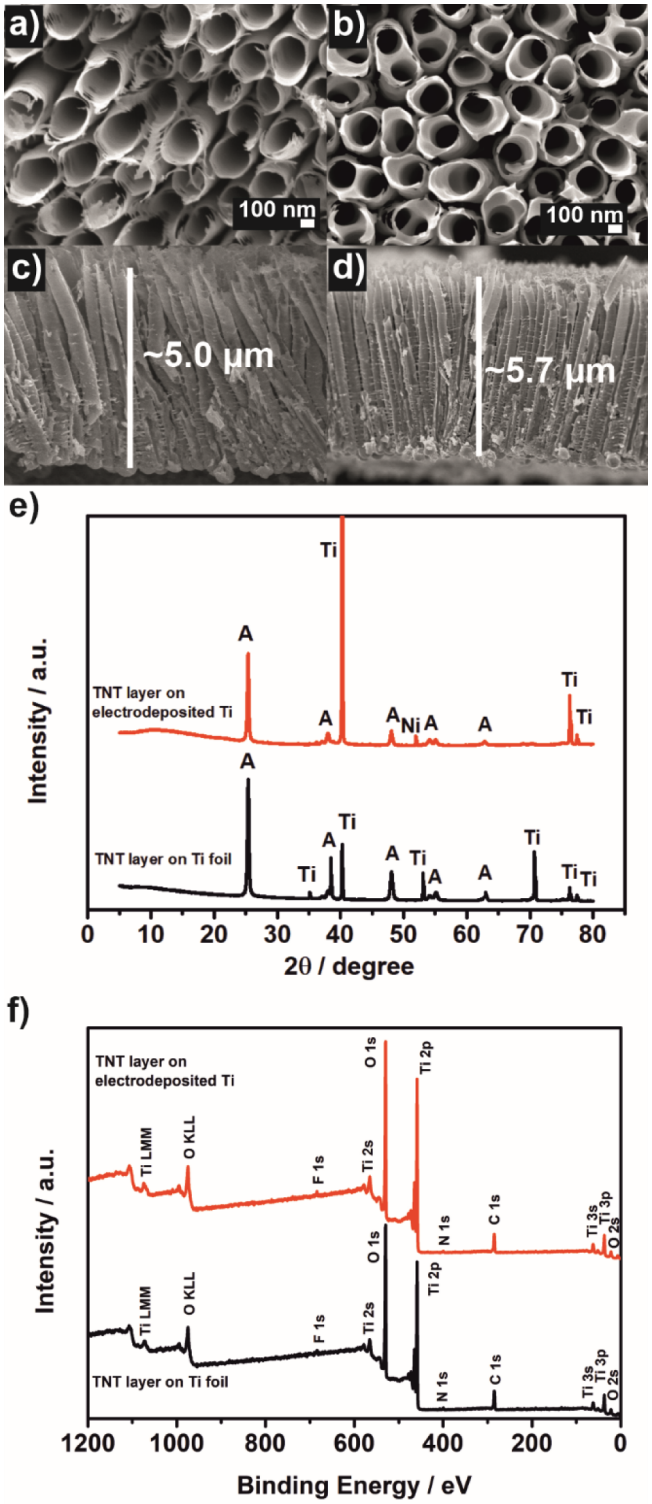

Fig. 2. (a-d) SEM images of the (a,b) nanotube tops and (c,d) cross sections of the TNT layers on (a,c) the electrodeposited Ti film and (b,d) the Ti foil. (e) XRD patterns and (f) XPS survey spectra.

for the (1 0 1) plane at approximately 25°, while the TNT layer on the Ti foil does not show any preferred orientation for the anatase TiO_2. The reason for this is that electrodeposited Ti film reveals a preferential orientation along the (1 0 1) plane of the α-titanium [23,25], whereas the rolled Ti foil does not have any such preferential orientation and shows a variety of planes. As a result, when these Ti materials are annealed, clear differences in the preferred orientation of anatase planes

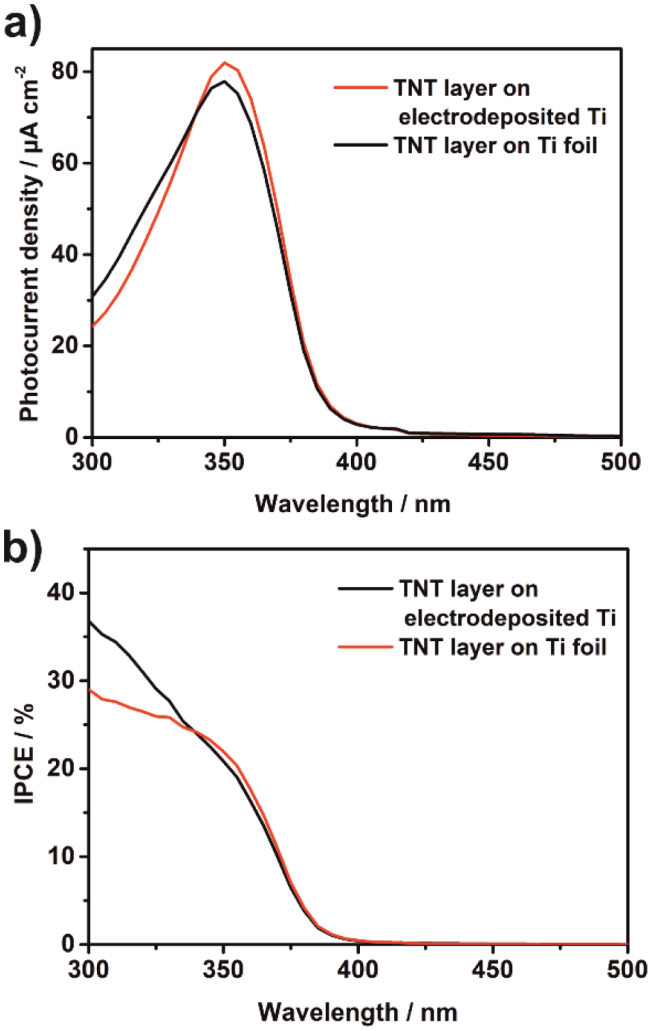

Fig. 3. (a) Photocurrent density and (b) corresponding IPCE values recorded on both TNT layers.

can be observed. The Ti signals (as well as the Ni signal in the case of the TNT layer on the electrodeposited Ti film) stem from the underlying substrates (i.e. Ti foil or Ti film electrodeposited on a Ni plate). The crystallite sizes for anatase, calculated by Scherrer's equation, are 477 Å and 467 Å for the TNT layers on the electrodeposited Ti film and the Ti foil, respectively.

XPS survey spectra for the TNT layers on both Ti substrates are shown in Fig. 2f. The ratios of O:Ti are 2.33 for the TNT layer on the electrodeposited Ti film and 2.22 for the TNT layer on the Ti foil. Thus, the stoichiometry of the TNT layer on the Ti foil is slightly better than that on the electrodeposited Ti film. The signals for F visible in the survey spectra stem from the electrolyte, while the C species can be attributed to adventitious carbon. Unlike the XRD results, no signal of Ni can be observed in the XPS spectrum of the TNT layer on the electrodeposited Ti film. The reason for this is that XPS is a surface sensitive characterization technique and the TNT layer is thick enough to avoid any interference from the underlying substrate. The absence of Ni species also means that the Ni substrate does not lead to any Ni contamination of the TNT layer.

Finally, Fig. 3 shows the photocurrent densities and the IPCE values measured for the TNT layers on both substrates. Both TNT layers show a maximum in photocurrent densities at a wavelength of ~350 nm. A slightly higher photocurrent density was recorded for the TNT layer on the electrodeposited Ti film compared to the TNT layer on the Ti foil. However, the increase is not substantial and it confirms previous

knowledge about TiO_2 nanotubes that for an optimal UV-photoresponse (i.e. interplay between the light absorption, charge carrier separation and mobility of electrons), their thickness must be in the range ~3 to 7 μm [29]. In this thickness range, the photocurrent response is saturated regardless of the exact thickness.

Thus, no significant differences were found between the TNT layers prepared on the electrodeposited Ti film and the Ti foil. As the electrodeposited Ti films are much thicker (and also cheaper) than the usual Ti films prepared by magnetron sputtering, and the anodization can be carried out for a longer time until all the Ti is consumed, electrodeposited Ti films could be a very promising potential substitute for the preparation of TNT layers. The TNT layers produced in this way also have no trace of the porous oxide layers found when using conductive glasses such as ITO or FTO as the substrate.

4. Conclusions

In conclusion, anodic TNT layers were prepared on electrodeposited Ti films for the first time. These TNT layers were compared to TNT layers produced on commonly used Ti foils using SEM, XRD, and XPS as well as photocurrent measurements. No significant differences were found between the TNT layers prepared on the two substrates, offering the possibility of using electrodeposited Ti layers instead of magnetron sputtered Ti layers.

CRediT authorship contribution statement

Hanna Sopha: Investigation, Methodology, Data curation, Writing - original draft, Writing - review & editing, Conceptualization. **Yutaro Norikawa:** Investigation, Writing - review & editing. **Martin Motola:** Investigation, Writing - review & editing. **Ludek Hromadko:** Visualization, Investigation, Writing - review & editing. **Jhonatan Rodriguez-Pereira:** Investigation, Data curation, Writing - review & editing. **Jiri Cerny:** Investigation, Data curation. **Toshiyuki Nohira:** Conceptualization, Funding acquisition, Writing - review & editing. **Kouji Yasuda:** Conceptualization, Funding acquisition, Writing - review & editing. **Jan M. Macak:** Conceptualization, Funding acquisition, Writing - review & editing.

Declaration of Competing Interest

The authors declare that they have no known competing financial interests or personal relationships that could have appeared to influence the work reported in this paper.

Acknowledgements

European Research Council (No. 638857) and the Ministry of Education, Youth and Sports of the Czech Republic (LM2018103, LQ1601) are acknowledged for the financial support of this work.

References

[1] K. Lee, A. Mazare, P. Schmuki, Chem. Rev. 114 (2014) 9385–9454, https://doi.org/10.1021/cr500061m.
[2] J.M. Macak, H. Tsuchiya, A. Ghicov, K. Yasuda, R. Hahn, S. Bauer, P. Schmuki, Curr. Opin. Solid State Mater. Sci. 11 (2007) 3–18, https://doi.org/10.1016/j.cossms.2007.08.004.
[3] P. Roy, S. Berger, P. Schmuki, Angew. Chemie Int. Ed. 50 (2011) 2904–2939, https://doi.org/10.1002/anie.201001374.
[4] J.M. Macák, H. Tsuchiya, P. Schmuki, Angew. Chemie Int. Ed. 44 (2005) 2100–2102, https://doi.org/10.1002/anie.200462459.
[5] A. Ghicov, H. Tsuchiya, J.M. Macak, P. Schmuki, Electrochem. Commun. 7 (2005) 505–509, https://doi.org/10.1016/j.elecom.2005.03.007.
[6] J.M. Macak, H. Tsuchiya, L. Taveira, S. Aldabergerova, P. Schmuki, Angew. Chemie Int. Ed. 44 (2005) 7463–7465, https://doi.org/10.1002/anie.200502781.
[7] J.M. Macak, P. Schmuki, Electrochim. Acta 52 (2006) 1258–1264, https://doi.org/10.1016/j.electacta.2006.07.021.
[8] J.M. Macak, M. Jarosova, A. Jäger, H. Sopha, M. Klementová, Appl. Surf. Sci. 371 (2016) 607–612, https://doi.org/10.1016/j.apsusc.2016.03.012.
[9] Z. Liu, V.R. Subramania, M. Misra, J. Phys. Chem. C 113 (2009) 14028–14033, https://doi.org/10.1021/jp903342s.
[10] M. Motola, L. Satrapinsky, T. Roch, Š. Jan, J. Kupčík, M. Klementová, M. Jakubičková, F. Peterka, G. Plesch, Catal. Today 287 (2017) 59–64, https://doi.org/10.1016/j.cattod.2016.10.011.
[11] J. Kapusta-Kołodziej, A. Chudecka, G.D. Sulka, J. Electroanal. Chem. 823 (2018) 221–233, https://doi.org/10.1016/j.jelechem.2018.06.014.
[12] J.M. Macak, H. Tsuchiya, S. Berger, S. Bauer, S. Fujimoto, P. Schmuki, Chem. Phys. Lett. 428 (2006) 421–425, https://doi.org/10.1016/j.cplett.2006.07.062.
[13] M. Motola, L. Satrapinskyy, M. Čaplovicová, T. Roch, M. Gregor, B. Grančič, J. Greguš, Ľ. Čaplovič, G. Plesch, Appl. Surf. Sci. 434 (2018) 1257–1265, https://doi.org/10.1016/j.apsusc.2017.11.253.
[14] J.E. Yoo, M. Altomare, M. Mokhtar, A. Alshehri, S.A. Al-Thabaiti, A. Mazare, P. Schmuki, Phys. Status Solidi Appl. Mater. Sci. 213 (2016) 2733–2740, https://doi.org/10.1002/pssa.201600140.
[15] H. Kmentova, S. Kment, L. Wang, S. Pausova, T. Vaclavu, R. Kuzel, H. Han, Z. Hubicka, M. Zlamal, J. Olejnicek, M. Cada, J. Krysa, R. Zboril, Catal. Today 287 (2017) 130–136, https://doi.org/10.1016/j.cattod.2016.10.022.
[16] S.L. Lim, Y. Liu, J. Li, E.-T. Kang, C.K. Ong, Appl. Surf. Sci. 257 (2011) 6612–6617, https://doi.org/10.1016/j.apsusc.2011.02.087.
[17] L. Wang, Y. Wang, Y. Yang, X. Wen, H. Xiang, Y. Li, RSC Adv. 5 (2015) 41120–41124, https://doi.org/10.1039/C5RA04893A.
[18] G.M. Haarberg, W. Rolland, Å. Sterten, J. Thonstad, J. Appl. Electrochem. 23 (1993) 217–224, https://doi.org/10.1007/BF00241912.
[19] X. Ning, H. Åsheim, H. Ren, S. Jiao, H. Zhu, Metall. Mater., Trans. B Process Metall. Mater. Process. Sci. 42 (2011) 1181–1187, https://doi.org/10.1007/s11663-011-9559-5.
[20] M.H. Kang, J. Song, H. Zhu, S. Jiao, Metall. Mater., Trans. B Process Metall. Mater. Process. Sci. 46 (2014) 162–168, https://doi.org/10.1007/s11663-014-0191-z.
[21] J. de Lepinay, J. Bouteillon, S. Traore, D. Renaud, M.J. Barbier, J. Appl. Electrochem. 17 (1987) 294–302, https://doi.org/10.1007/BF01023295.
[22] A. Robin, J. De Lepinay, M.J. Barbier, J. Electroanal. Chem. 230 (1987) 125–141, https://doi.org/10.1016/0022-0728(87)80137-7.
[23] Y. Norikawa, K. Yasuda, T. Nohira, Mater. Trans. 58 (2017) 390–394, https://doi.org/10.2320/matertrans.MK201605.
[24] Y. Norikawa, K. Yasuda, T. Nohira, Electrochemistry 86 (2018) 99–103, https://doi.org/10.5796/electrochemistry.17-00082.
[25] Y. Norikawa, K. Yasuda, T. Nohira, J. Electrochem. Soc. 166 (2019) D755–D759, https://doi.org/10.1149/2.1291914jes.
[26] S. Das, H. Sopha, M. Krbal, R. Zazpe, V. Podzemna, J. Prikryl, J.M. Macak, ChemElectroChem 4 (2017) 495–499, https://doi.org/10.1002/celc.201600763.
[27] H. Sopha, L. Hromadko, K. Nechvilova, J.M. Macak, J. Electroanal. Chem. 759 (2015) 122–128, https://doi.org/10.1016/j.jelechem.2015.11.002.
[28] S. Das, R. Zazpe, J. Prikryl, P. Knotek, M. Krbal, H. Sopha, V. Podzemna, J.M. Macak, Electrochim. Acta 213 (2016) 452–459, https://doi.org/10.1016/j.electacta.2016.07.135.
[29] R.P. Lynch, A. Ghicov, P. Schmuki, J. Electrochem. Soc. 157 (2010) G76–G84, https://doi.org/10.1149/1.3276455.